G. Bhanuprakash Reddy*, P. Yadagiri Reddy and Avadhesha Surolia*

Alzheimer's and Danish dementia peptides induce cataract and perturb retinal architecture in rats

DOI 10.1515/bmc-2016-0025
Received September 15, 2016; accepted December 8, 2016

Abstract: Familial Danish dementias (FDDs) are autosomal dominant neurodegenerative disorders that are associated with visual defects. In some aspects, FDD is similar to Alzheimer's disease (AD)– the amyloid deposits in FDD and AD are made of short peptides: amyloid β (Aβ) in AD and ADan in FDD. Previously, we demonstrated an interaction between the dementia peptides and α-crystallin leading to lens opacification in organ culture due to impaired chaperone activity of α-crystallin. Herein, we report the *in vivo* effects of ADan and Aβ on the eye. ADan [reduced (ADan-red) and oxidized (ADan-oxi)] and Aβ (Aβ1-40 and Aβ1-42) were injected intravitreally in rats. The onset of cataract was seen after injection of all the peptides, but the cataract matured by 2 weeks in the case of ADan-red, 5 weeks for ADan-oxi and 6 weeks for Aβ1-40, while Aβ1-42 had minimal effect on cataract progression. The severity of cataract is associated with insolubilization and alterations in crystallins and loss of chaperone activity of α-crystallin. Further, disruption of the architecture of the retina was evident from a loss of rhodopsin, increased gliosis, and the thinning of the retina. These results provide a basis for the dominant heredo-otoophthalmo-encephalopathy (HOOE)/FDD syndrome and indicate that ADan peptides are more potent than Aβ peptides in inflicting visual impairment.

Keywords: α-crystallin; ADan; amyloid β; cataract; Danish dementia.

Introduction

Improved technology and health and nutrition have led to increased lifespan, which in turn has contributed to the growth of aging populations (1). With the rise in the average age of the population, there is an increased risk of chronic diseases such as diabetes, cancer, cardiovascular disorders, and neurodegenerative diseases, leading to disability and related mortality (2–4). Neurodegenerative diseases are becoming increasingly common, resulting in a greater burden on the health care system of most countries. Many of these bewildering disorders are known to arise from the conformational instability leading to protein misfolding and aggregation (5, 6). Conformational diseases arise when a constituent protein undergoes a change in size or fluctuation in shape, with resultant self-association and tissue deposition. There are at least a dozen diseases known to arise from protein misfolding or aggregation, which have potentially devastating medical and social consequences (5–7). Normally, these protein deposits are aggregates of mostly β-pleated sheets with distinct morphological features. Such changes can occur with normal proteins as well, but there is usually an interacting genetic contribution which is at times the dominant force. Most of these proteins have pivotal roles in the signaling cascade and cell cycle control, which result in large-scale health consequences upon their instability.

Cataract, characterized by cloudiness or opacification of the eye lens, is the leading cause of blindness all over the world (8). Crystallins are the major structural proteins in the lens whose structure, stability, and short-range interactions are important for lens transparency (9, 10). The human lens is also susceptible to age-related degenerative changes such as accumulation of insoluble proteins and oxidative damage (10). There are three distinct crystallins: α-, β-, and γ-crystallins. α-Crystallin, a member of the small heat shock protein family, constitutes a major portion of the eye lens cytoplasm and exists as a hetero-oligomer with two subunits, αA and αB (9–12). Increased levels of αB-crystallin have been observed in many neurodegenerative disorders, tumors, and diabetic conditions (13, 14). Both these proteins are known for their chaperone activity (9, 11, 12, 15, 16) and presumably protect other lens proteins from the adverse effects of various cataractogenic insults. With ageing, eye lens proteins undergo various post-translational modifications, which mostly lead to their aggregation. Various physiological, environmental, and genetic factors accelerate this aggregation and predispose the lens to cataract

***Corresponding authors: G. Bhanuprakash Reddy,** Biochemistry Division, National Institute of Nutrition, Hyderabad 500007, Telangana, India, e-mail: bhanu@icmr.org.in; and **Avadhesha Surolia,** Molecular Biophysics Unit, Indian Institute of Science, Bengaluru 560012, Karnataka, India, e-mail: surolia@mbu.iisc.ernet.in
P. Yadagiri Reddy: Biochemistry Division, National Institute of Nutrition, Hyderabad, India

formation (10, 17). Retinal degenerations (RD), a group of heterogeneous diseases of the retina, are characterized by photoreceptor degeneration and retinal pigment epithelium atrophy, causing loss of visual field and acuity, resulting in irreversible blindness (18). More than 200 genes have been implicated in RD [Retinal Information Network (RetNet), https://sph.uth.tmc.edu/retnet/]. Mutations leading to the altered conformation of proteins have been shown to be the underlying cause of several dominant neurodegenerative diseases, including dominant retinitis degenerations. Protein misfolding leading to altered trafficking and aggregation are common features of these conditions (19, 20).

Defects in the *BRI2* gene on chromosome 13 leads to two autosomal dominant neurodegenerative disorders, i.e. familial British dementias and familial Danish dementias (FBDs and FDDs) (21, 22). While the onset of FBD usually occurs in the fifth decade of life with progressive dementia, spasticity, and ataxia, the onset of FDD ensues earlier, before 30 years of age, with cataracts and visual loss followed by impaired hearing, progressive cerebellar ataxia, and late dementia (22–24). Histological signatures of FDD are cerebral amyloid angiopathy, parenchymal protein deposits, and neurofibrillary degeneration (22, 25–27). Also, parenchymal amyloid deposits and neurofibrillary tangles are consistently found with significant destruction of the hippocampal region. In this regard, FDD is closely similar to Alzheimer's disease (AD), the major cause of dementia in aging populations. Also, in both the cases, amyloid deposits are made of short peptides generated in the brain by the internal proteolysis of large transmembrane precursor proteins. These peptides of ~4 kDa are amyloid β (Aβ) in AD (28, 29), and ADan in FDD (21, 22). In FDD, a 10-nucleotide duplication-insertion causes a frame shift and the generation of the ADan sequence (22). FDD is also known as heredo-otoophthalmo-encephalopathy (HOOE). HOOE/FDD is a dominantly inherited syndrome clinically characterized by a gradual loss of vision, deafness, progressive ataxia, and dementia (24, 30). Retinal neovascularization and posterior subscapular cataract in FDD cause visual loss in FDD. Cataracts seem to be the earliest manifestation of this disease, starting at the age of 20, followed by hearing impairment developing at the age of 40. Interestingly, early onset of cataract is also seen in Alzheimer's and Down syndrome patients (31).

Various studies now have shown a role for Aβ in RD (32). Both the oxidized (linked by an intramolecular disulfide bond) and the reduced (no intramolecular disulfide bond present) forms of ADan peptides fail to produce fibres at pH 7.0 (25). Nonetheless, previously we reported that the form of the peptides determines the morphology of the aggregates (33). We also reported that the reduced form is more neurotoxic than the oxidized form (33–35). Further, we demonstrated the interaction between dementia-associated peptides and α-crystallin, which impaired the chaperone activity of α-crystallin (7). Interestingly, it was found that the ADan-reduced peptide (ADan-red) has both exquisite specificity and ability amongst several amyloidogenic peptides to compromise the chaperone function of α-crystallin. Moreover, the correlation between the poisoning of the chaperone activity and loss of lens transparency in organ culture by the pathogenic form of the Danish dementia peptides provided an explanation for the high incidence of the occurrence of cataract in Danish dementia (7). In the present study, we have investigated the effect of ADan (both reduced and oxidized) and Aβ (Aβ1-40 and Aβ1-42) on the lens and retina in animals upon intravitreal injection.

Results

Onset and progression of cataract

The onset of cataract due to peptide injection was observed in rats after 1 week of intravitreal injection and progressed to mature cataract by 2–6 weeks (Figure 1). The averaged stage of cataract at the given time in a given group is shown in Figure 1B. The onset of cataract was seen 1 week after intravitreal injection of ADan-red and the ADan-oxidized form (ADan-oxi). While the cataract matured by 2 weeks in the case of ADan-red, it took 5 weeks to mature in the case of ADan-oxi. In the case of Aβ1-40, the onset of cataract was observed after 2 weeks, which progressed to maturation by 6 weeks. However, with Aβ1-42, the onset of cataract occurred after 4 weeks and it progressed to only stage 1.5 of cataract by 6 weeks. All the contralateral lenses injected with DMSO as a vehicle appeared to be normal and free of opacities during the experimental period. Based on the trajectories of onset and progression of lens abnormalities, the potential of peptides inducing cataract *in vivo* in these studies was found to be in the order of ADan-red, ADan-oxi, Aβ1-40, and Aβ1-42.

Protein content

We analyzed the total and soluble protein content in the lens, as insolubilization and aggregation of soluble

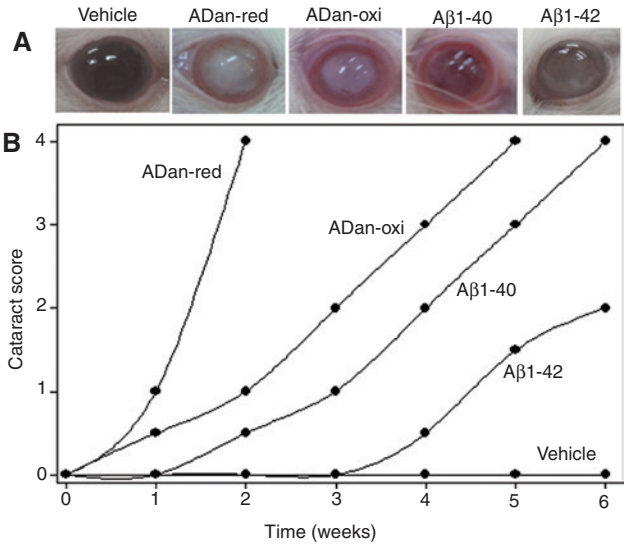

Figure 1: Induction of cataract upon intravitreal injection of dementia peptides.
(A) Representative photographs of the lens from each group. (B) Quantitative representation of cataract progression in each group with time. Stage of cataract in each group was averaged at a given time and plotted as a function of time (n = 7).

Table 1: Protein content of the lens.

Peptides	Total protein (mg/g lens)	Soluble protein (mg/g lens)	% Soluble protein
ADan-red			
DMSO	615 ± 43	491 ± 30	80
Peptide	524 ± 38	305 ± 28[a]	58
ADan-oxi			
DMSO	605 ± 42	481 ± 31	79
Peptide	505 ± 34	313 ± 30[a]	62
Aβ1-40			
DMSO	602 ± 46	475 ± 33	79
Peptide	519 ± 40	345 ± 26[a]	66
Aβ1-42			
DMSO	590 ± 37	478 ± 29	81
Peptide	495 ± 32	347 ± 26[a]	70

The total and soluble protein in the lens of different groups was estimated by the Lowry method, and the percentage soluble protein content was derived from the estimated values.
The data are mean ± SE (n = 4).
[a]Data are significantly different from those of the respective control (DMSO) group.

lens proteins lead to cataractogenesis. The percentage of soluble protein decreased to 58%–70% in the lenses injected with peptides as compared to 80% of soluble protein in vehicle-injected lenses (Table 1). The decline in the percentage of soluble protein was highest in lenses injected with ADan-red and modest with Aβ1-42. These results indicate that increased insolubilization (decreased soluble protein) is associated with the severity of cataract in dementia-injected lenses.

Crystallin distribution and protein cross-links

The soluble protein fractions were analyzed by HPLC on an SEC column and SDS-PAGE. The lens-soluble fraction was clearly resolved into α-, β-, and γ-crystallin peaks on the SEC column (Figure 2). While there were alterations in crystallin peaks in ADan-red-, ADan-oxi-, and Aβ1-40-injected lenses compared to vehicle-injected lenses (Figure 2), the crystallin distribution profile of Aβ1-42-injected lenses was similar to that of vehicle-injected lenses (Figure 2). The decrease in β- and γ-crystallin peaks, particularly in the ADan-red and ADan-oxi lenses, suggests that the oligomerization of crystallins in the peptide-induced cataract lenses may be involved in the formation of aggregates due to cross-linking, which leads to their insolubilization. The

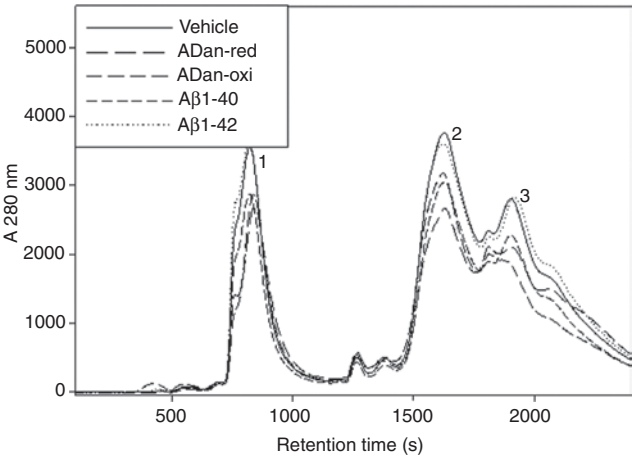

Figure 2: Crystallin profile of total soluble lens protein on gel filtration.
Proteins from control (vehicle)-, ADan-red-, ADan-oxi-, Aβ1-40-, and Aβ1-42-injected eye lenses were loaded onto the column. The column was equilibrated, the proteins were eluted with the buffer, and absorbance was monitored at 280 nm. The traces are the average of four samples in each group. Peaks 1, 2 and 3 correspond to α-, β- and γ-crystallins, respectively.

SDS-PAGE pattern of soluble protein (Figure 3) showing an increased proportion of cross-linked and aggregated proteins in the peptide-injected lenses compared with the vehicle-injected lenses substantiates the HPLC data. The SDS-PAGE pattern of Aβ1-42-injected lenses was similar to that of vehicle-injected lenses (Figure 3).

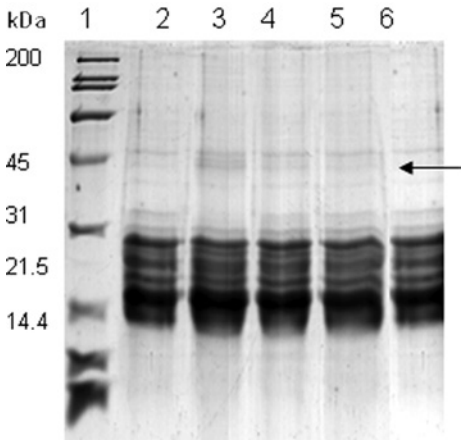

Figure 3: Representative sub-unit profile and protein cross-linking of the soluble fraction of dementia peptide-injected lenses.
Lane 1: markers, lane 2: DMSO, lane 3: ADan-red, lane 4: ADan-oxi, lane 5: Aβ1-40, and lane 6: Aβ1-42. The arrow indicates cross-linked proteins in the peptide-injected lens under reducing conditions.

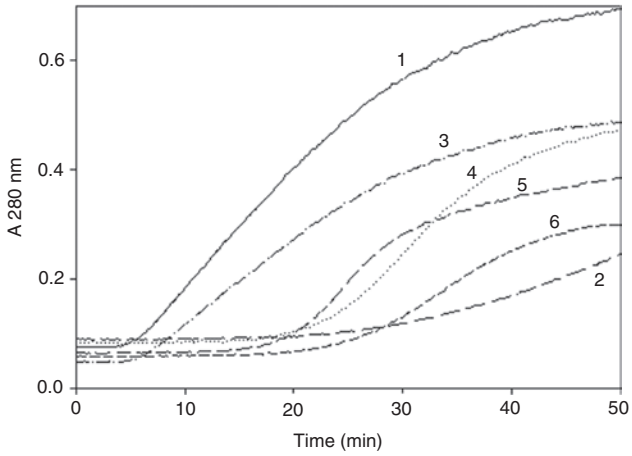

Figure 4: Chaperone activity of α-crystallin as assessed by the suppression of heat-induced aggregation of citrate synthase at 45°C in the absence (trace 1) and presence of α-crystallin isolated from the lenses injected with vehicle (trace 2), ADan-red (trace 3), ADan-oxi (trace 4), Aβ1-40 (trace 5), and Aβ1-42 (trace 6).
The traces are the average of four samples in each group.

Chaperone activity of α-crystallin

α-Crystallin isolated from the rat lenses treated with ADan-red showed significantly decreased (58%) chaperone activity as compared to α-crystallin isolated from vehicle-injected lenses in the citrate synthase aggregation assay (Figure 4). In comparison, the reduction in chaperone activity of α-crystallin isolated from lenses treated with ADan-oxi, Aβ1-40 peptide, and Aβ1-42 was 54%, 43%, and 31%, respectively (Figure 4).

Changes in retinal morphology upon intravitreal injection of the ADan and Aβ peptides

We also evaluated retinal morphology by hematoxylin and eosin (H and E) staining the sections of the retina from rats injected with DMSO and dementia peptides (Figure 5). The retinas from rats injected with peptides showed significant alterations. The integrity of the retina from the ADan-red-injected rat was severely affected. ADan-red led to reduced thickness of the outer segment (OS), the outer nuclear layer (ONL), and the inner nuclear layer (INL). Further, there was a disruption of ONL and no clear demarcation between the ONL and the INL in the retina of ADan-red-treated animals. Further histological evaluation of the retina demonstrated abnormalities in the INL in the peptide-injected eyes. Also, the thickness of the outer plexiform layer (OPL) and the inner plexiform layer (IPL) was observed to be decreased in the peptide-injected retina compared to controls. While similar alterations were observed in ADan-oxi and Aβ1-40 retinas, the retinal pattern of Aβ1-42 was not much different from that of the respective DMSO control. These results suggest that dementia peptides, particularly ADan-red, disrupt the integrity of the retina in a profound manner.

Immunohistochemical analysis of rat retina was carried out using the antibodies to the major retinal photoreceptor protein rhodopsin. Immunostaining with rhodopsin antibodies showed a significant reduction in the intensity of the rhodopsin signal in the retina of rats injected with dementia peptides compared with that of DMSO controls (Figure 6). The decrease in rhodopsin intensity was highest with ADan-red, followed by ADan-oxi and Aβ1-40. The rhodopsin staining of Aβ1-42 sections was similar to that of the DMSO control. To further confirm alterations in the retina, we evaluated and compared the immunoreactivity by labeling the retina with glial marker GFAP. Gliosis in retinal Müller cells is characterized by the increased expression of the immunoreactivity of GFAP. This increased immunoreactivity of GFAP suggests the induction of retinal reactive gliosis in dementia-peptide injected eyes (Figure 7). In the present study, the observed increased expression of GFAP is suggestive of local inflammation. In concurrence with histological changes, injection of ADan-red caused greater changes in rhodopsin and GFAP followed by ADan-oxi and Aβ1-40, whereas the impact was least with Aβ1-42.

Discussion

Familial British dementia (FBD) and familial Danish dementia (FDD) are autosomal dominant neurodegenerative

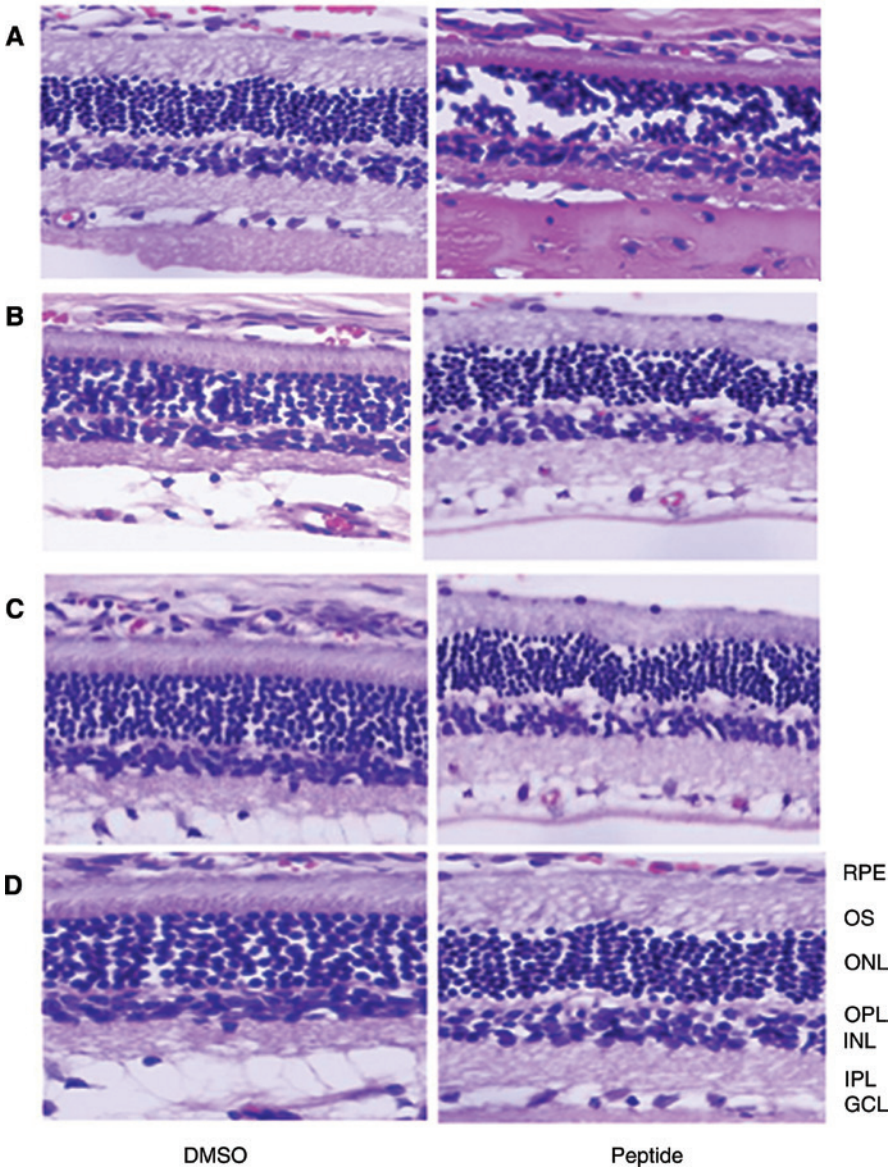

Figure 5: Morphology of the retina.
Representative histology (hematoxylin and eosin stained) images of rat retina. Panel A: ADan-red; panel B: ADan-oxi; panel C: Aβ1-40; and panel D: Aβ1-42.

disorders associated with mutations in the gene *BRI2*. In pathological aspects, FDD is closely similar to AD. Further, FDD and AD produce similar amyloid deposits that are made of short peptides generated in the brain by internal proteolysis of precursor proteins. FDD is characterized by a gradual loss of vision and dementia, among many other symptoms, and the loss of vision is mainly due to posterior subcapsular cataract and retinal neovascularization (24, 30). Recent studies indicate visual defects involving the lens and the retina during the development of AD (31, 32). Earlier, we showed loss of eye lens transparency in organ culture when incubated with ADan peptides wherein there was a remarkable correlation between the ability of the ADan peptides to impair the chaperone activity of α-crystallin *in vitro* and opacification of the eye lenses *ex vivo* (7). Other dementia-related peptides, despite their established role in amyloid diseases, exhibit relatively poor inhibition of the chaperone function of eye lens crystallins as well as considerably less opacification of lenses in organ culture compared to the ADan-red peptide, explaining why in FDD alone, among the amyloid diseases, an early onset of cataract is observed. However, it should be noted that the Aβ1-40 peptide is known to be expressed in rodent and monkey lenses and oxidative stress has been shown to increase the production of the Aβ precursor protein and Aβ1-40 (36). It was demonstrated that Aβ has toxic effects on lens epithelial cells (36).

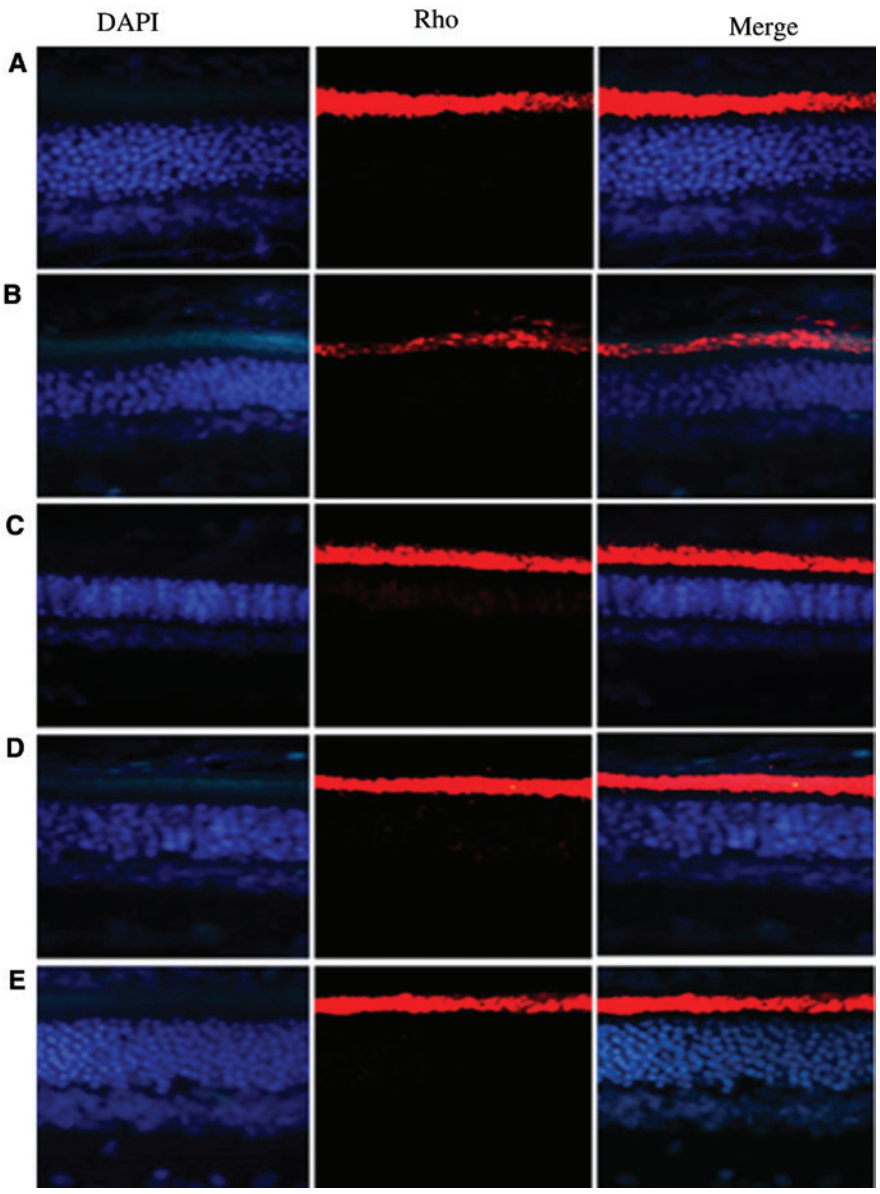

Figure 6: Immunohistochemical evaluation of the rod photoreceptor marker rhodopsin.
Representative retinal sections of control- (A), ADan-red- (B), ADan-oxi- (C), Aβ1-40- (D), and Aβ1-42- (E) injected eyes that were labeled with rhodopsin (red). Nuclei are labeled with DAPI (blue). Scale bar: 50 μm.

Further, Aβ was also shown to interact with αB-crystallin (37, 38). Similarly, retinal ganglion cells (RGC) and the retinal pigment epithelial (RPE) cells were also reported to synthesize and secrete Aβ (39). In the eye, multiple Aβ reservoirs were discovered in the retinal environment, while elevated Aβ levels were found in the aging retina and linked with retinal degeneration (32, 39).

In this study, we attempted to provide a molecular basis for the role of ADan and Aβ under *in vivo* conditions upon intravitreal injection into rat eyes. Interestingly, the ability of peptides to induce cataract *in vivo* in these studies correlated with their potential to impair chaperone activity of the α-crystallins *in vitro* and loss of lens transparency in the *ex vivo* conditions reported earlier (7). Aggregation of soluble lens proteins leading to insolubilization is the main biochemical change in cataractogenesis. Injection of dementia peptides also resulted in insolubilization (decreased soluble protein), which is associated with the severity of cataract. Altered crystallin distribution and cross-linking of their subunits further support induction of cataract upon injection of peptides. Though various other factors may contribute to aggregation, insolubilization of lens proteins and reduced chaperone activity of α-crystallin appear to be the major determinants in cataract formation

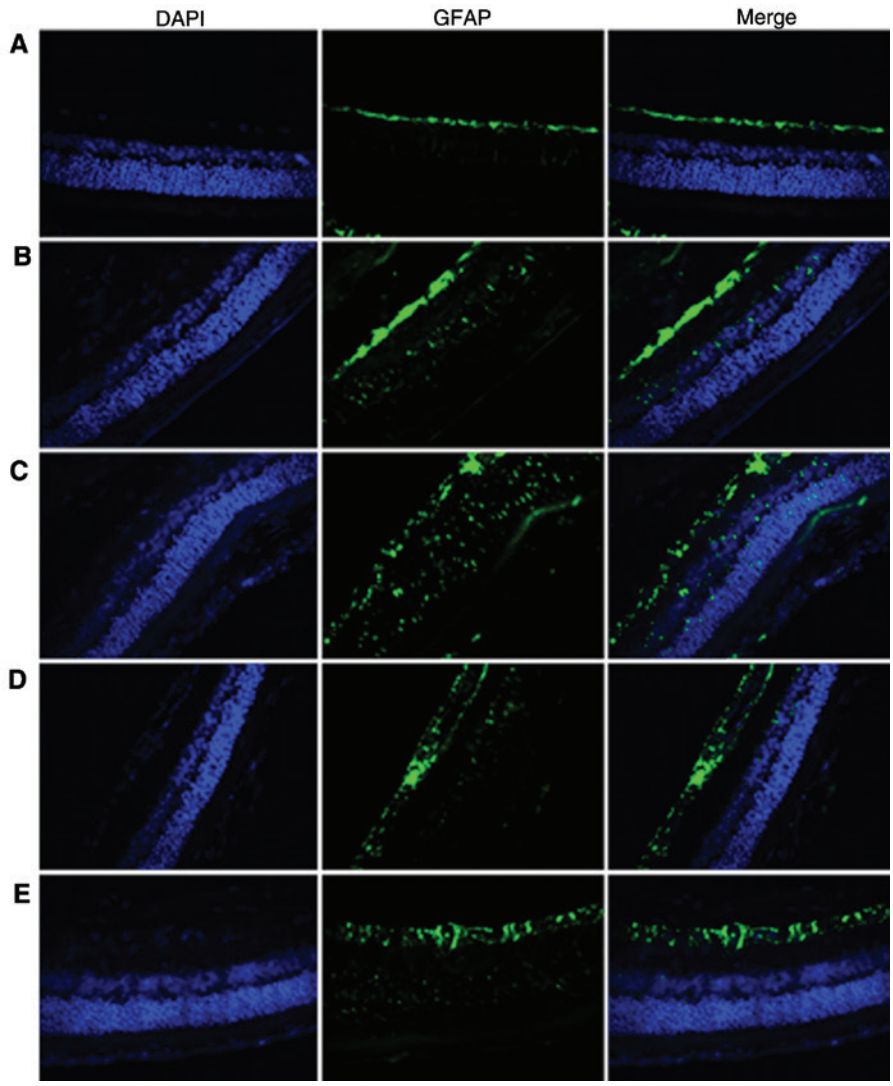

Figure 7: Immunohistochemical evaluation of gliosis marker glial fibrillary acidic protein (GFAP).
Representative retinal sections of control- (A), ADan-red- (B), ADan-oxi- (C), Aβ1-40- (D), and Aβ1-42- (E) injected eyes that were labeled with GFAP (green). Nuclei are labeled with DAPI (blue). Scale bar: 50 μm.

in peptide-injected lenses. As reported by us previously (7), binding of dementia peptides may impair the chaperone activity of α-crystallin.

Both the retina and the central nervous system (CNS) share a common origin as both are derived from the developing neural tube. Both are interconnected with the adjacent vasculature via the blood-retinal and blood-brain barriers. Furthermore, with increasing age, both the retina and the brain develop extracellular deposits associated with degenerative pathology, referred to as drusen and senile plaques, respectively. Inflammatory mediators that are indicative of local inflammation typically associated with sub-retinal deposits and senile plaques are also common in the retina and CNS (32, 39). These similarities between the retina and the CNS suggest that similar pathological mechanisms may drive degenerative changes in the retina as well as in the brain. Though some studies have proposed a role for Aβ peptides in RD (32, 39), the effect of the Danish dementia peptide on the retina is largely unknown. Therefore, we have also examined the retinal morphology upon intravitreal injection of ADan peptides along with Aβ peptides. Interestingly, it was observed that the integrity of the retina upon injection of ADan peptides was relatively more affected compared to injection of Aβ peptides. On the whole, the thickness of various layers of the retina was reduced. Further, there was a disruption of the ONL and no clear demarcation between the ONL and the INL in the retina of ADan-red treated animals. Further histological evaluation of the retina demonstrated abnormalities in the INL in the peptide-injected eyes. Also, the thickness of the OPL and

the IPL was observed to be decreased in the peptide-injected retina compared to controls. While similar alterations were observed in ADan-oxi and Aβ1-40 retinas, the retinal pattern of Aβ1-42 was not very different from that of the respective DMSO control. Moreover, immunohistochemical analysis of rat retinas showed a significant reduction in the rhodopsin signal in the retina of rats injected with ADan and Aβ1-40 peptides compared to DMSO controls. Gliosis in retinal Müller cells as shown by increased immunoreactivity of the GFAP by dementia peptide is further suggestive of local inflammation. These results suggest that dementia peptides, particularly the ADan-red peptide, disrupt the integrity of the retina in a profound manner.

It is, therefore, not surprising that the many striking similarities between drusen and senile plaques include Aβ. However, it is interesting to note that ADan peptides are more potent than Aβ peptides in disrupting the retina. Overall, the potential of peptides causing visual impairment (both lens and retina) *in vivo* in these studies was found in the order of ADan-red, ADan-oxi, Aβ1-40, and Aβ1-42. Further, these results provide a mechanistic basis for the dominant HOOE/FDD syndrome viz. the poisoning of the chaperone-like function of α-crystallins. Studies that report the role of α-crystallin in other neurodegenerative conditions support this possibility (15). Such studies have found a correlation of amyloidogenic properties of the ADan protein with the initiation of neuronal cell death mechanisms that involve oxidative stress, perturbation of mitochondrial membrane potential, the release of mitochondrial cytochrome c, and downstream activation of caspase-mediated apoptotic pathways (40). For example, it is reported that α-crystallins mediate transport of newly synthesized rhodopsin by binding to the photoreceptor post-Golgi membranes (41) and this association of α-crystallins with rhodopsin imply a role for α-crystallins in the protection of neurodegeneration. Together, with our earlier studies that reported the neurotoxicity of ADan (33–35), these results highlight that ADan peptides contribute not only to cataract but also to retinal dystrophies through their neurotoxic effects. Further, these observations suggest that ADan peptides are more potent than Aβ peptides regarding visual impairment.

Materials and methods

Materials

Danish dementia peptides (ADan-red and ADan-oxi) and Alzheimer's peptides (Aβ1-40 and Aβ1-42) were bought from Bachem AG (Bubendorf, Switzerland) and purified using a C-18 HPLC column, and the purity and mass of the peptides were assessed by a MALDI-TOF mass spectrometer (BrukerDaltonics, MA, USA) as described earlier (7, 33). The peptides were subjected to a 1, 1, 1, 3, 3, 3-hexafluoro-2-propanol (HFIP) treatment as described earlier (7, 33). The lyophilized peptides thus obtained were dissolved in dimethyl sulphoxide (DMSO) under a flow of liquid nitrogen. While the sequence of ADan-red is 'ASNCFAIRHFENKFAVETLICFNLFLNSQEKHY', there is a disulfide bond between Cys4 and Cys21 in ADan-oxi. The sequence of Aβ1-42 is 'DAEFRHDSGYEVHHQKLVFFAEDVGSNKGAIIGLMVGGVVIA' and Aβ1-40 is devoid of last two C-terminal residues.

Animals

Twenty-eight 4-month-old Sprague-Dawley (SD) male rats were obtained from the National Center for Laboratory Animal Sciences (NCLAS), National Institute of Nutrition, Hyderabad. The rats were maintained at NCLAS in a temperature- and light-controlled animal facility and fed *ad libitum* on a rodent pellet diet (AIN-93M).

Intravitreal injection

The animals were randomly divided into four groups (7 animals per group). Peptides (10 μg in 5 μl) were injected into the vitreous of the right (R) eye and the same volume of vehicle (DMSO) into the left (L) eye on day 0. Three more injections were given on every third day. Immediately after each intravitreal injection, ofloxacin ophthalmic solution was applied onto the eyes to avoid infection.

Slit-lamp examination of the eye lens

Eyes were examined every week using a slit lamp biomicroscope (Kowa SL-15 Portable, Tokyo, Japan) on dilated pupils. Initiation and progression of lenticular opacity were graded into four categories as reported earlier (42). The animals were maintained for a period of six weeks.

Collection of tissues

The rats were sacrificed by CO_2 asphyxiation after 6 weeks and the eyes were enucleated. A set of eyeballs (n = 4) were dissected using the posterior approach, and the lens and the retina were frozen at – 80°C until further analysis. Another set of eyeballs (n = 3) were collected in 4% w/v paraformaldehyde fixative solution for histology and immunohistochemistry.

Animal care and protocols were approved by the Institutional Animal Ethics Committee and conformed to the Association for Research in Vision and Ophthalmology statement for the use of animals in ophthalmic and vision research.

Protein solubility, crystallin distribution, protein crosslinking, and protein aggregation

A 10% homogenate was made from the lenses in 50 mM phosphate buffer, pH 7.4. The homogenate was centrifuged at 10000 × g for

30 min at 4°C. The supernatant was referred to as the soluble fraction. The pellet was washed twice with 50 mM phosphate buffer, pH 7.4, and the wash was pooled with the supernatant. Total and soluble protein content were estimated in the homogenate and soluble fractions by the Lowry method, and the percentage of soluble protein was calculated. An aliquot of total homogenate was solubilized in 0.1 N sodium hydroxide containing 2% sodium carbonate for estimating the total protein. An aliquot of soluble fraction was applied onto a 300 × 7.8-mm TSK-3000 SW-XL size exclusion chromatography (SEC) column (Tosoh Co., Tokyo, Japan) connected to a Shimadzu HPLC system. The subunit profile and cross-linking of lens soluble proteins were analyzed on 12% polyacrylamide gels in the presence of sodium dodecyl sulfate (SDS) under reducing conditions.

Chaperone-like activity assay

The soluble fraction was applied onto a Sephacryl S-300 HR (Pharmacia Biotech, Uppsala, Sweden) column equilibrated with a 25-mM Tris-Cl buffer, pH 8.0, containing 0.5 mM EDTA and 100 mM NaCl. The peak corresponding to αL-crystallin was pooled and dialyzed extensively against the buffer (7). Proteins were concentrated by ultrafiltration using 10 K filters (Millipore Pvt., Ltd., Bangalore, India). The chaperone-like activity of α-crystallin was probed by measuring its ability to prevent the heat-induced aggregation of citrate synthase at 45°C (7, 15). Citrate synthase (0.05 mg/ml in 50 mM HEPES-KOH buffer, pH 7.9) was incubated at 45°C in the absence and presence of 0.05 mg/ml α-crystallin. Apparent scattering of the solution at 360 nm due to the heat-induced aggregation of citrate synthase was monitored as a function of time using a spectrophotometer (Lambda-35, Perkin-Elmer, MA, USA).

Histology and immunohistochemistry

Eyeballs were collected from the animals and fixed in 4% paraformaldehyde in phosphate buffer (pH 7.2), followed by embedding and sectioning using standard protocols, as described previously (43, 44). Three eyes were used for each age group. Paraffin sections were stained with hematoxylin and eosin. Immunohistochemistry was performed on sections using a respective primary antibody, as described previously (43, 44). The slides were mounted in the antifade reagent containing DAPI (ProlongGold; Invitrogen) and visualized using a Leica laser microscope (LMD6000; Leica Microsystems Vertrieb GmbH, Wetzlar, Germany).

Acknowledgments: A.S. is a Bhatnagar Fellow of the Council of Scientific and Industrial Research (CSIR), India. This work was partially supported by a grant from CSIR to A.S. and by the Department of Biotechnology and Department of Science and Technology, Government of India, to G.B.R. We thank Dr. V. Sudhakar Reddy and Ms. Sneha Jakhotia, National Institute of Nutrition, Hyderabd, for the criticial discussion and help in the preparation of the manuscript.

List of abbreviations

Aβ	amyloid β
AD	Alzheimer's disease
FDD	familial Danish dementias
HOOE	heredo-otoophthalmo-encephalopathy

References

1. Partridge L. Intervening in ageing to prevent the diseases of ageing. Trends Endocrinol Metab 2014; 25: 555–7.
2. Fontana L, Partridge L, Longo VD. Extending healthy life span-from yeast to humans. Science 2010; 328: 321–6.
3. Piper MD, Partridge L, Raubenheimer D, Simpson SJ. Dietary restriction and aging: a unifying perspective. Cell Metab 2011; 14: 154–60.
4. DG dCRLC. The biology of aging in Harrison's principles of Internal medicine, Columbus, OH, USA: McGraw-Hill Education, 2015.
5. Dobson CM. Protein misfolding, evolution and disease. Trends Biochem Sci 1999; 24: 329–32.
6. Carrell RW, Lomas DA. Conformational disease. Lancet 1997; 350: 134–8.
7. Surolia I, Sinha S, Sarkar DP, Reddy PY, Reddy GB, Surolia A. Concurrence of Danish dementia and cataract: insights from the interactions of dementia associated peptides with eye lens alpha-crystallin. PLoS One 2008; 3: e2927.
8. Pascolini D, Mariotti SP. Global estimates of visual impairment. Br J Ophthalmol 2010; 96: 614–8.
9. Reddy GB, Kumar PA, Kumar MS. Chaperone-like activity and hydrophobicity of alpha-crystallin. IUBMB Life 2006; 58: 632–41.
10. Bloemendal H, de Jong W, Jaenicke R, Lubsen NH, Slingsby C, Tardieu A. Ageing and vision: structure, stability and function of lens crystallins. Prog Biophys Mol Biol 2004; 86: 407–85.
11. Horwitz J. Alpha-crystallin. Exp Eye Res 2003; 76: 145–53.
12. Srinivas PN, Reddy PY, Reddy GB. Significance of alpha-crystallin heteropolymer with a 3:1 alphaA/alphaB ratio: chaperone-like activity, structure and hydrophobicity. Biochem J 2008; 414: 453–60.
13. Reddy VS, Reddy GB. Emerging role for alphaB-crystallin as a therapeutic agent: pros and cons. Curr Mol Med 2015; 15: 47–61.
14. Reddy VS, Reddy GB. Role of crystallins in diabetic complications. Biochim Biophys Acta 2016; 1860: 269–77.
15. Reddy GB, Das KP, Petrash JM, Surewicz WK. Temperature-dependent chaperone activity and structural properties of human alphaA- and alphaB-crystallins. J Biol Chem 2000; 275: 4565–70.
16. Kumar MS, Kapoor M, Sinha S, Reddy GB. Insights into hydrophobicity and the chaperone-like function of alphaA- and alphaB-crystallins: an isothermal titration calorimetric study. J Biol Chem 2005; 280: 21726–30.
17. Kumar PA, Reddy GB. Modulation of alpha-crystallin chaperone activity: a target to prevent or delay cataract? IUBMB Life 2009; 61: 485–95.
18. Daiger SP, Bowne SJ, Sullivan LS. Perspective on genes and mutations causing retinitis pigmentosa. Arch Ophthalmol 2007; 125: 151–8.

19. Saliba RS, Munro PM, Luthert PJ, Cheetham ME. The cellular fate of mutant rhodopsin: quality control, degradation and aggresome formation. J Cell Sci 2002; 115: 2907–18.
20. Vasireddy V, Chavali VR, Joseph VT, Kadam R, Lin JH, Jamison JA, Kompella UB, Reddy GB, Ayyagari R. Rescue of photoreceptor degeneration by curcumin in transgenic rats with P23H rhodopsin mutation. PLoS One 2011; 6: e21193.
21. Vidal R, Frangione B, Rostagno A, Mead S, Revesz T, Plant G, Ghiso J. A stop-codon mutation in the BRI gene associated with familial British dementia. Nature 1999; 399: 776–81.
22. Vidal R, Revesz T, Rostagno A, Kim E, Holton JL, Bek T, Bojsen-Moller M, Braendgaard H, Plant G, Ghiso J, Frangione B. A decamer duplication in the 3′ region of the BRI gene originates an amyloid peptide that is associated with dementia in a Danish kindred. Proc Natl Acad Sci U S A 2000; 97: 4920–5.
23. Mead S, James-Galton M, Revesz T, Doshi RB, Harwood G, Pan EL, Ghiso J, Frangione B, Plant G. Familial British dementia with amyloid angiopathy: early clinical, neuropsychological and imaging findings. Brain 2000; 123: Pt 5: 975–91.
24. Stromgren E, Dalby A, Dalby MA, Ranheim B. Cataract, deafness, cerebellar ataxia, psychosis and dementia--a new syndrome. Acta Neurol Scand 1970; 46: Suppl 43: 261+.
25. Gibson G, Gunasekera N, Lee M, Lelyveld V, El-Agnaf OM, Wright A, Austen B. Oligomerization and neurotoxicity of the amyloid ADan peptide implicated in familial Danish dementia. J Neurochem 2004; 88: 281–90.
26. Holton JL, Lashley T, Ghiso J, Braendgaard H, Vidal R, Guerin CJ, Gibb G, Hanger DP, Rostagno A, Anderton BH, Strand C, Ayling H, Plant G, Frangione B, Bojsen-Moller M, Revesz T. Familial Danish dementia: a novel form of cerebral amyloidosis associated with deposition of both amyloid-Dan and amyloid-beta. J Neuropathol Exp Neurol 2002; 61: 254–67.
27. Holton JL, Ghiso J, Lashley T, Rostagno A, Guerin CJ, Gibb G, Houlden H, Ayling H, Martinian L, Anderton BH, Wood NW, Vidal R, Plant G, Frangione B, Revesz T. Regional distribution of amyloid-Bri deposition and its association with neurofibrillary degeneration in familial British dementia. Am J Pathol 2001; 158: 515–26.
28. Glenner GG, Wong CW. Alzheimer's disease: initial report of the purification and characterization of a novel cerebrovascular amyloid protein. Biochem Biophys Res Commun 1984; 120: 885–90.
29. Masters CL, Simms G, Weinman NA, Multhaup G, McDonald BL, Beyreuther K. Amyloid plaque core protein in Alzheimer disease and Down syndrome. Proc Natl Acad Sci U S A 1985; 82: 4245–9.
30. Bek T. Ocular changes in heredo-oto-ophthalmo-encephalopathy. Br J Ophthalmol 2000; 84: 1298–302.
31. Goldstein LE, Muffat JA, Cherny RA, Moir RD, Ericsson MH, Huang X, Mavros C, Coccia JA, Faget KY, Fitch KA, Masters CL, Tanzi RE, Chylack LT Jr, Bush AI. Cytosolic beta-amyloid deposition and supranuclear cataracts in lenses from people with Alzheimer's disease. Lancet 2003; 361: 1258–65.
32. Ratnayaka JA, Serpell LC, Lotery AJ. Dementia of the eye: the role of amyloid beta in retinal degeneration. Eye (Lond) 2015; 29: 1013–26.
33. Surolia I, Reddy GB, Sinha S. Hierarchy and the mechanism of fibril formation in ADan peptides. J Neurochem 2006; 99: 537–48.
34. Surolia I, Sarkar DP, Sinha S. Form and dimensions of aggregates dictate cytotoxicities of Danish dementia peptides. Biochem Biophys Res Commun 2008; 372: 62–6.
35. Surolia I, Chhibber M, Sarkar DP, Sinha S. Fibrillogenesis in ADan peptides is inhibited by biphenyl ethers. Biochem Biophys Res Commun 2008; 370: 681–6.
36. Frederikse PH, Ren XO. Lens defects and age-related fiber cell degeneration in a mouse model of increased AbetaPP gene dosage in Down syndrome. Am J Pathol 2002; 161: 1985–90.
37. Liang JJ. Interaction between beta-amyloid and lens alphaB-crystallin. FEBS Lett 2000; 484: 98–101.
38. Stege GJ, Renkawek K, Overkamp PS, Verschuure P, van Rijk AF, Reijnen-Aalbers A, Boelens WC, Bosman GJ, de Jong WW. The molecular chaperone alphaB-crystallin enhances amyloid beta neurotoxicity. Biochem Biophys Res Commun 1999; 262: 152–6.
39. Lacor PN, Buniel MC, Furlow PW, Clemente AS, Velasco PT, Wood M, Viola KL, Klein WL. Abeta oligomer-induced aberrations in synapse composition, shape, and density provide a molecular basis for loss of connectivity in Alzheimer's disease. J Neurosci 2007; 27: 796–807.
40. Todd K, Ghiso J, Rostagno A. Oxidative stress and mitochondria-mediated cell death mechanisms triggered by the familial Danish dementia ADan amyloid. Neurobiol Dis 2016; 85: 130–43.
41. Deretic D, Aebersold RH, Morrison HD, Papermaster DS. Alpha A- and alpha B-crystallin in the retina. Association with the post-Golgi compartment of frog retinal photoreceptors. J Biol Chem 1994; 269: 16853–61.
42. Saraswat M, Suryanarayana P, Reddy PY, Patil MA, Balakrishna N, Reddy GB. Antiglycating potential of Zingiber officinalis and delay of diabetic cataract in rats. Mol Vis 2010; 16: 1525–37.
43. Reddy GB, Vasireddy V, Mandal MN, Tiruvalluru M, Wang XF, Jablonski MM, Nappanveettil G, Ayyagari R. A novel rat model with obesity-associated retinal degeneration. Invest Ophthalmol Vis Sci 2009; 50: 3456–63.
44. Reddy VS, Raghu G, Reddy SS, Pasupulati AK, Suryanarayana P, Reddy GB. Response of small heat shock proteins in diabetic rat retina. Invest Ophthalmol Vis Sci 2013; 54: 7674–82.